

Solar Ultraviolet Variability Over Time Periods of Aeronomic Interest

Thomas N. Woods and Gary J. Rottman

Laboratory for Atmospheric and Space Physics, University of Colorado, Boulder, Colorado.

The solar ultraviolet (UV) radiation is a primary energy source for planetary atmospheres and is also a tool for remote sensing of the planets. The solar UV radiation from mostly below 300 nm dissociates molecules, ionizes the neutral atmosphere, and affects many chemical cycles in the atmospheres. In addition, solar photons scatter off the molecules and atoms in the atmospheres and provide a method of remote sensing the composition and density of the atmospheres. For such aeronomic studies, accurate values of the solar UV irradiance, primarily shortward of 200 nm, are needed over time periods of days to decades. A planet's orbital motion around the Sun and the intrinsic solar variability are the primary causes of the variation of the solar intensity at a planet. The insolation changes caused by the orbital motion are easily calculated as the inverse square of the Sun-planet distance; however, the intrinsic solar irradiance variability is more complicated and is strongly dependent on wavelength and time. The primary short-term irradiance variability over several days is caused by the solar rotation, which has a mean period of 27 days. The primary long-term variability is related to the solar dynamo that reverses the solar magnetic field and is known as the 11-year solar cycle. The variations observed during solar cycle 22 (1986-1996) are the basis for creating some reference spectra of the solar UV irradiance for use in comparative aeronomic studies. From these reference spectra, the solar cycle variability as a function of wavelength can be characterized as 15% and less at wavelengths longward of 160 nm, as 15% to 70% between 160 and 65 nm, and as a factor of 1.5 to 7 between 65 and 1 nm. The magnitude of the 27-day rotational variability is usually no more than one third of the solar cycle variability. There is not a smooth transition of variability between wavelengths, but instead the amount of intrinsic solar variability depends on the source of the radiation in the solar atmosphere. In general, the coronal emissions vary the most, then the transition region emissions vary somewhat less, chromospheric emissions vary even less, and finally the photospheric emissions vary the least, perhaps only 0.1% at the longest UV wavelengths.

INTRODUCTION

The solar ultraviolet (UV) radiation, being wavelengths less than 400 nm, is an important source of energy for aeronomic processes throughout the solar system. The solar

UV photons are absorbed in planetary and cometary atmospheres, as well as throughout the heliosphere, via photodissociation of molecules, photoionization of molecules and atoms, and photoexcitation including resonance scattering (e.g., see *Chamberlain* [1978]). The subdivisions of the UV spectral range for this discussion include the near ultraviolet (NUV) as the 300 to 400 nm range, the middle ultraviolet (MUV) as the 200 to 300 nm range, the far ultraviolet (FUV) as the 120 to 200 nm range, the extreme ultraviolet (EUV) as the 30 to 120 nm range, the x-ray ultraviolet (XUV) as the 1 and 30 nm range, and x-rays as wavelengths less than 1 nm. The solar EUV and XUV radiation photoionizes the neutral constituents of the atmospheres and participates in the formation of the ionosphere. The photoelectrons created in this process interact further with the neutrals, leading to excitation, dissociation, and additional ionization. The excess energy from the absorption processes goes into heating the atmosphere. As an example for Earth as shown in Plate 1, the solar MUV radiation heats the stratosphere, and the solar UV radiation shortward of 170 nm heats the thermosphere. The absorption of the solar UV radiation also initiates many chemical cycles in the atmospheres, such as the chemistry of water vapor, ozone, and nitric oxide in Earth's atmosphere (e.g., see *Brasseur and Solomon* [1986]). As depicted in Plate 1, the chemistry cycle of ozone in Earth's stratosphere is balanced largely by the creation of ozone via the photodissociation of molecular oxygen followed by the combination of the atomic oxygen with molecular oxygen and by the destruction of ozone via direct photodissociation. The longer wavelengths of the solar radiation, mainly from the NUV, visible (VIS: 400-700 nm), and near infrared (NIR: 700-10000 nm), are absorbed by aerosols, clouds, and gases in the troposphere and by land surfaces and oceans; thus, the Sun also affects those environments. All of these atmospheric processes are wavelength dependent and are expected to be as variable as the intrinsic solar variability at the appropriate wavelengths. Therefore, accurate measurements of the solar UV spectral irradiance, along with an understanding of its variability, are important for detailed studies of the aeronomic processes.

The remote sensing of the composition and density in the heliosphere, comets, and planetary atmospheres is often determined by measuring the brightness of an emission that is created by the resonant scattering of solar UV photons. In particular, the column density of a constituent is often derived by dividing the measured brightness of the emission by the g-factor, or fluorescence efficiency. The g-factor is based on well-known atomic parameters, such as the emission's oscillator strength, and the incident solar irradiance (e.g., see *Meier* [1995]). Consequently, the accuracy of the derived abundance is directly dependent on the accuracy

of the emission brightness measurement and on the accuracy of the solar UV irradiance, both spectral intensity and shape. Often there are not cotemporal measurements of the solar UV irradiance, so estimates must be used in the analysis. These estimates may be calculated or derived from measurements taken at other times but projected to the desired epoch. Reference spectra of the solar UV irradiance are presented here to aid such aeronomic studies.

The solar UV irradiance can be incorporated in a variety of ways into studies of comparative aeronomy. For detailed studies of aeronomic observations, cotemporal observations of the solar UV irradiance provide the most accurate solar information. Reference spectra of the solar UV irradiance, which are normally based on actual observations, are sometimes included in aeronomic studies, for example, to determine the sensitivity of an aeronomic model to solar variability. In cases where solar observations are not available or have incomplete wavelength coverage, which is often the case for the EUV and XUV, models of the solar irradiance can provide an estimate of the solar spectrum for a given aeronomic observation. These models can be as simple as linear scaling between two reference spectra or complicated physical models of the solar irradiance. The focus here is on the general behavior of the Sun and not on any specific aeronomic study; therefore, reference solar irradiance spectra, along with a discussion of the present understanding of the solar variability, are the focus for this paper. For more detailed information about the historical background and previous results of the solar UV irradiance, one should examine reviews, for example, by *White* [1977], *Rottman* [1987], *Lean*, [1987 and 1991], *Tobiska* [1993], and *Pap et al.* [1994].

SOLAR SPECTRUM

The overall solar spectrum is fairly well characterized as a continuum similar to a blackbody with a temperature near 5800 °K. The radiation peaks near 600 nm and falls slowly and continuously toward the longer infrared wavelengths, but falls quite abruptly toward the shorter wavelengths of the ultraviolet. Moreover, for the UV wavelengths the spectrum is not smooth but is superimposed in the UV longward of 200 nm with strong absorption lines (Fraunhofer lines) and absorption edges that make the spectrum deviate from the smooth blackbody curve. Shortward of 200 nm the spectrum changes from having absorption lines to having emission lines, and by 130 nm the solar spectrum is dominated more by emission lines than by the continuum. These emission lines arise from the dominant species, H and He, and the many minor species in the higher layers of the solar atmosphere as a non-local thermodynamic equilibrium (non-LTE) effect and are strongly

sensitive to the magnetic activity on the Sun. These emissions also include the ionization continua, such as the bright H ionization continuum shortward of 91 nm. These general characteristics of the solar UV spectrum are evident in Plate 2, which includes a solar spectrum at 0.1 nm spectral resolution. This spectrum and others discussed here are the solar spectral irradiance, which is the spectral radiance (or intensity) at a single wavelength integrated over the full-disk of the Sun and observed at a distance of 1 AU. Most of the discussion here focuses on the UV shortward of 200 nm because it is the spectral range especially important for solar-aeronomy studies. This spectral range is commonly called the vacuum UV (VUV) because measurements shortward of 200 nm require a vacuum, such as from space, and the VUV is often subdivided into the XUV, EUV, and FUV ranges as shown in Plate 2.

The continuum is emitted mainly from the photosphere, and the many emission features are emitted from the solar upper atmosphere: chromosphere, transition region, and corona. The dominant species, H and He, contribute much of the irradiance, such as the bright H I Lyman- α (121.6 nm) and He II Lyman- α (30.4 nm) emissions. The distribution of the emission features with wavelength is based on the complex atomic energy levels of the source gases. To generalize the emission spectral distribution, the higher temperature emissions arising from the more highly ionized atoms naturally have higher energy states and thus occur at shorter wavelengths. For example, the solar radiation shortward of 20 nm is dominated by coronal emissions. With the density decreasing with altitude and the temperature increasing at higher layers of the solar atmosphere, the radiation from the higher layers is, in general, more variable. In other words, the coronal emissions vary more than the transition region emissions, which in turn vary more than the chromospheric emissions.

SOURCES OF SOLAR VARIABILITY

For studies of comparative aeronomy two aspects of the solar irradiance are important: one is the absolute value of the irradiance, and the second is its variability. Both aspects are considered here, but the absolute value of the irradiance is deferred to a later discussion. The value of the solar intensity incident on a solar system body will vary for three reasons: (1) changes in the distance to the Sun, (2) changes in the radiation field directed from the Sun toward the body, and finally, (3) intrinsic variation in the output of the Sun.

Considering first the distance to the Sun, the solar intensity at a planet varies inversely as the distance squared. The resulting change in intensity is generally called insolation as it is not an intrinsic variation of the solar radiation. Table 1 lists some important orbital characteristics for the

nine planets. One of the columns in Table 1 lists the " $\langle 1/R^2 \rangle$ Effect", which is the inverse of the average Sun-planet distance squared; these values are normalized to unity for Earth, which has a mean Earth-Sun distance of 1 AU. For this discussion, the solar irradiance is considered the full-disk solar intensity at 1 AU. As an example, the intensity relative to the irradiance at Earth is a factor of 2 at Venus, 1% at Saturn, and 0.1% at Neptune. The column labeled " ϵ -Effect" is the orbital eccentricity effect and lists the insolation variation encountered during a planet's motion about the Sun, and the column "Orbital Period" provides the corresponding time base of this variation. For example, the Earth's orbital eccentricity ($\epsilon = 0.017$) gives rise to a 7% insolation variation with a period of one year. In January the insolation is 7% larger while the Earth is at perihelion than in June when it is at aphelion. Likewise, Jupiter experiences about 20% insolation variation due to its orbital motion with a period of about 12 years, quite close to the 11-year solar cycle variation. Therefore, in the case of Jupiter the orbital changes in the insolation may overwhelm the intrinsic solar cycle irradiance variations at certain wavelengths, while at other wavelengths the solar cycle variations may overwhelm the orbital changes.

The second variation of solar intensity that a planet is certain to experience is due to a "search-light" effect resulting from the non-uniform distribution of bright regions on the solar disk that are modulated by the 27-day rotation period of the Sun. Regardless of whether the solar disk has many bright active regions or only a few and if the distribution of these features is non-uniform, as is usually the case, the 27-day variation of irradiance is quite apparent. If the solar irradiance is measured from Earth, then these values are only appropriate to celestial bodies in opposition (or inferior conjunction for inner planets) with the Earth. Bodies at other solar longitudes experience a time record of irradiance advanced or retarded by an appropriate phase. Fortunately, features on the Sun appear and disappear over a period of a few months, so the irradiance time series can be considered quasi-stationary, often allowing phase (time) shifts up to $\pm 180^\circ$ with reasonable confidence.

The third type of solar variation, and the one considered in more detail in this paper, is intrinsic or inherent solar variability. The magnetic activity on the Sun is the primary cause of the intrinsic solar variability and is manifested into a variety of features on the solar disk. The plagues, active network, and quiet network are a generalization of the principle features on the Sun that affect the variability of the solar UV radiation. These solar features are defined for modeling purposes and are described in more detail by Schrijver [1988], Harvey and White [1999], and Worden *et al.* [1998]. The plagues are the large, bright active regions observable in the UV, as can be seen in the so-

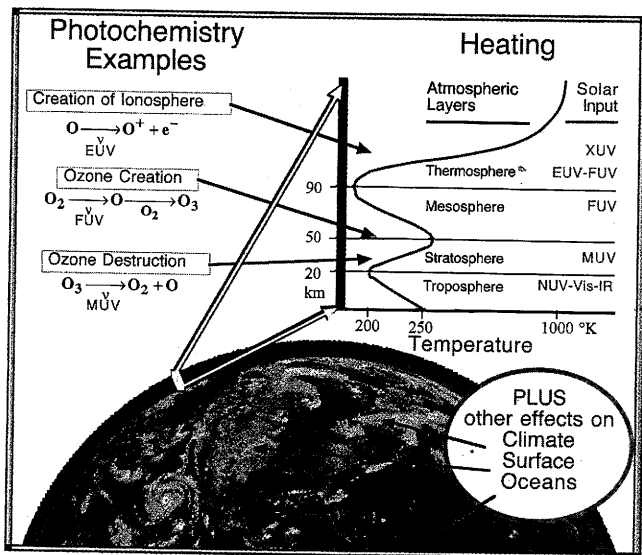


Plate 1. The solar UV radiation is a primary energy input to Earth's atmosphere. This radiation includes the middle UV (MUV: 200-300 nm), the far UV (FUV: 120-200 nm), the extreme UV (EUV: 30-120 nm), and the x-ray UV (XUV: 1-30 nm). The photochemistry and heating of the atmosphere vary with altitude and are strongly dependent on the wavelength of the solar radiation and the absorption cross sections of the atmospheric species.

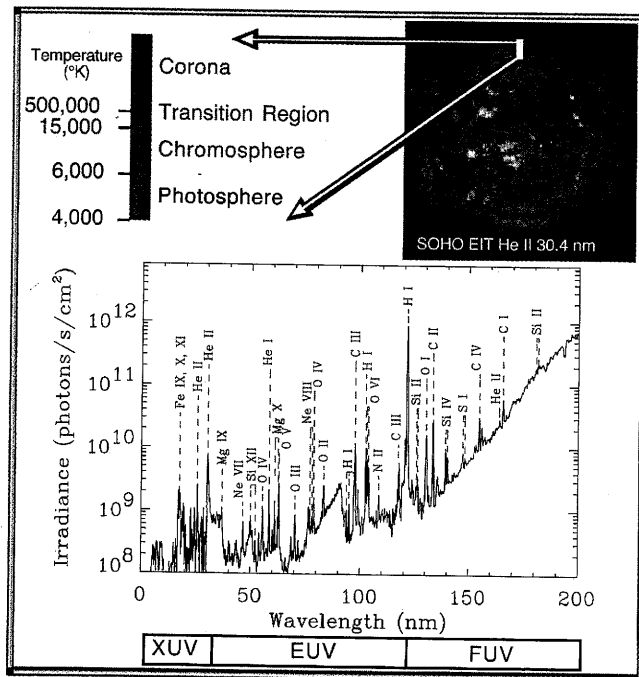


Plate 2. The solar UV irradiance shortward of 200 nm is dominated by emissions from the chromosphere, transition region, and corona layers of the solar atmosphere. A few of the brighter emissions are labeled in the spectrum using the color coding of the solar atmospheric layers shown above.

Table 1. The variations of the solar intensity due to orbital motion changes are listed for the planets where R is the distance to the Sun and ϵ is the orbital eccentricity.

Planet	$\langle 1/R^2 \rangle$ Effect (1 = Earth)	ϵ Effect (%)	Orbit Period (yr)
Mercury	6.75	130	0.24
Venus	1.93	3.0	0.62
Earth	1	6.9	1.00
Mars	0.43	45	1.88
Jupiter	0.037	21	11.9
Saturn	0.011	25	29.5
Uranus	0.0027	21	84
Neptune	0.0011	3.7	164
Pluto	0.00064	178	248

lar image in Plate 2, and are associated with the dark sunspots and bright faculae features seen in the visible. The plages are intense, localized regions that appear primarily below 30° latitude on the Sun, and as a collective group their rotation with the solar atmosphere produces a strong 27-day rotational variability. The active network is the decay of the plages into smaller, more diffuse regions over a period of a few months. The active network is distributed almost uniformly over the solar longitudes and, consequently, has only a weak, if any, contribution to the 27-day variability. The quiet network is often assumed to have constant radiance regardless of the solar activity, although some recent results indicate that the quiet network may vary with the solar cycle [Schühle *et al.*, 2000]. During a solar cycle, the plage fractional area over the solar disk varies from 0 to 0.2, and the active network fractional area varies from 0.04 to 0.2 [Worden *et al.*, 1998 and 1999]. The quiet network fractional area is simply one minus the plage and active network fractional areas. It is important to note that the active network fractional area is not zero during solar minimum; therefore, the solar minimum irradiance is probably at slightly different levels during different solar cycles [Worden *et al.*, 1998]. Lean *et al.* [1982] and Worden [1996] have successfully used the area of these three components, namely plage, active network, and quiet network, to model the variability of the solar UV irradiance. Moreover, they have shown that at least these three components are needed to explain both the 27-day variability and the 11-year variability observed in the solar UV irradiance, and moreover, that emissions at different wavelengths have different sensitivities to these three components. Related to this later point, Woods *et al.* [2000b] have shown that the 11-year variability of the transition region emissions, such as the H I Lyman- α (121.6 nm) emission, has a much larger contribution from the active

network regions than so for the long-term variability of the chromospheric or coronal emissions. As a summary for intrinsic solar variability, both the different layers of the solar atmosphere and the composition of features on the solar disk are needed to study the solar variability as a function of wavelength.

TIME PERIODS OF SOLAR VARIABILITY

The Sun varies over all time periods, and the amount of variability is a strong function of wavelength. The irradiance variations most important for aeronomic studies include minute-long flares, the 27-day solar rotation, and the 11-year solar cycle. Very short-term variations, lasting from minutes to hours, are related to eruptive phenomena on the Sun, short-term variations, modulated by the 27-day rotation period of the Sun, are related to the appearance and disappearance of active regions on the solar disk, and the prominent long-term solar cycle variability is related to the 22-year magnetic field cycle of the Sun caused presumably by the internal solar dynamo.

The eruptive events, such as flares, occur over time periods of a few minutes. The flare emissions are most often seen in the coronal emissions; therefore, the solar flares predominantly alter the shorter XUV wavelengths, which in turn affect more the plasma (via ionization) than the neutrals in a planetary atmosphere. There are a few large flares during a solar cycle that do have a large impact on the full-disk irradiance at many wavelengths and thus can cause detectable atmospheric changes. The GOES 1-8 Å x-ray measurements clearly show several flares per month with increases of irradiance by factors of 10 to 1000, but only two large flares have been detected in the FUV irradiance during the first 9 years of the UARS mission (1991-2000), due in large part to the UARS duty cycle and observing mode. Brekke *et al.* [1996] report increases of the transition region emissions by a factor of 12 for a very extended X3.3 class flare on February 27, 1992. A large increase, a factor of 3, of the transition region emissions was also observed for a very extended X5.7 class flare on July 14, 2000. During these large flare events the chromospheric emissions and the FUV continuum also showed increases by factors of 1.3 to 2 and 1.1 to 1.5, respectively. Because of the infrequent occurrences of large flares, it is difficult to generalize the flare irradiance as a function of wavelength.

The solar rotation of about 27-days is a strong component in the irradiance variation at essentially all wavelengths. The Sun is a differential rotator with its equator rotating with a period of about 24 days and the higher latitudes rotating more slowly with a period of about 30 days. When a single active region or a set of regions localized in

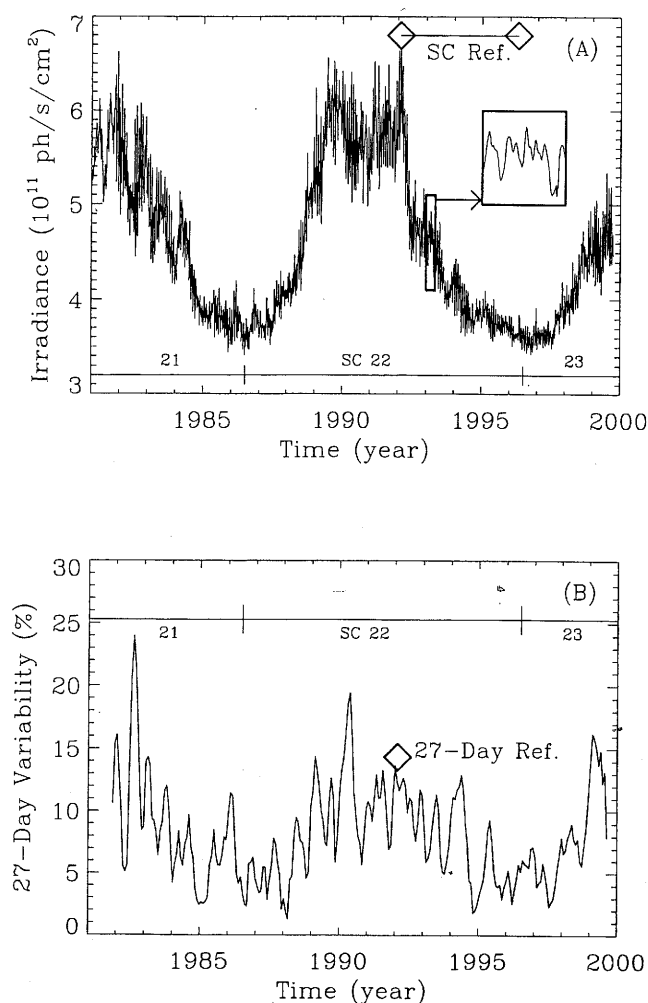


Figure 1. The irradiance time series (panel A) and the amplitudes of the 27-day variability (panel B) are shown for the H I Lyman- α (121.6 nm) irradiance during the past 20 years. The primary variations are the 27-day rotational variation and the 11-year solar cycle. The amplitude of the 27-day variability changes throughout the solar cycle. The diamond symbols in panels A and B indicate the time periods selected for the solar cycle 22 reference spectra and 27-day reference variability, respectively.

longitude dominates the Sun, the irradiance has a strong rotation variability whose period is partially dependent on the solar latitude of the primary active regions. This strong rotational variability is often maintained for a few months as active regions evolve slowly. The formation of new active regions appear somewhat random; however, there are usually 1 or 2 major outbursts each year that give rise to a strong rotation variability. This variability is referred to as the 27-day variation after the mean period found from Fourier spectral analysis of the solar irradiance time series.

The period of this variability does range from 22 to 35 days due to the differential rotation of the Sun and the location of the different active regions on the Sun. The magnitude of 27-day variability for the H I Lyman- α (121.6 nm) emission is shown in Figure 1 over solar cycles 21 and 22. These short-term variations are larger during solar maximum conditions because there are more active regions during solar maximum. While many chromospheric and coronal emissions, such as F10.7, have little or no short-term variations during solar minimum conditions, the transition region emissions, such as the H I Lyman- α , usually have short-term variations throughout solar minimum.

The variations of the solar irradiance over many months and years, referred to as long-term variability, is related to the reversal of the global magnetic field on the Sun, presumably caused by the solar dynamo deep within the solar interior [e.g., Layden *et al.*, 1991, Levy, 1992]. This magnetic reversal has a full cycle of about 22 years, but, with the radiation intensity varying with the magnetic field amplitude and independent of polarity, the irradiance variability has a period of about 11 years, referred to as the 11-year solar cycle. The solar dynamo cycle has even longer variability periods, perhaps cyclic with periods of 88 years and longer [Feynman and Gabriel, 1990]. The movement of the sunspots over a solar cycle is explained by Spörer's law [Spörer 1894] and is illustrated by the well-known "butterfly diagram" by Maunder [1922] and Babcock [1961]. A new 11-year solar cycle is first detected by pairs of new cycle sunspots appearing at moderately high solar latitudes ($\sim 30^\circ$) with their magnetic field orientation (north-south) opposite from sunspots of the previous solar cycle. New cycle active regions usually first appear during solar minimum while old cycle active regions are still present near the solar equator. As the solar cycle progresses toward the next solar maximum, the differential rotation of the Sun effectively pulls the active regions towards the solar equator. Consequently, the new active regions are generated at lower latitudes as the 11-year cycle progresses. The latitudinal distribution of the active regions over a solar cycle has a peak near $\pm 10^\circ$; also, the time when the active regions are centered near $\pm 10^\circ$ latitude roughly corresponds to the time of solar maximum. Approaching solar minimum the active regions are mostly near the equator.

OBSERVATIONS

Because the solar VUV radiation is absorbed entirely in Earth's atmosphere, its observations did not begin until the start of the space research era in the late 1940s. One of the first research rockets included a solar UV spectrometer [Baum *et al.*, 1946], and these early observations clearly showed that the Sun had significant UV emissions in ex-

cess of its blackbody continuum. Following these early rocket measurements, several satellite programs beginning in the 1960s included solar UV irradiance instruments. Some of the pioneering missions included the Orbiting Solar Observatory (OSO) -3 and -4, [Hall and Hinteregger, 1970; Reeves and Parkinson, 1970], a series of Solar Radiation (SOLRAD) spacecraft [Kreplin, 1970; Kreplin and Horan, 1992], and the Atmospheric Explorer (AE) -C, -D, and -E [Hinteregger et al., 1973]. Most of these early missions were NASA satellites supported by the Air Force Cambridge Research Laboratories (AFCRL), the Naval Research Laboratory (NRL), and the University of Colorado (CU). With this new era of UV measurements from space, each observation was significant in showing both the magnitude of the irradiance and its possible variability. As more observations were made, it became clear that instrument pre-flight calibrations and analysis of in-flight instrument degradation needed to be improved because instrumental effects on the order of 30-100% often obscured the solar variability. The more recent solar measurements from the Upper Atmosphere Research Satellite (UARS) have addressed this issue by including two independent instruments that have accurate pre-flight calibrations traceable to the National Institute of Standards and Technology (NIST) radiometric standards and also have in-flight calibrations to precisely track instrument degradation.

Improved solar irradiance measurements are expected for solar cycle 23 from the new observations by the NASA Thermosphere Ionosphere Mesosphere Energetics and Dynamics (TIMED) and Solar Radiation and Climate Experiment (SORCE) satellites. The TIMED Solar EUV Experiment (SEE) will provide solar irradiances from 1 to 195 nm with ~10% accuracy [Woods et al., 1998b]. The TIMED launch is currently planned for the Fall 2001. The SORCE satellite contains 4 solar irradiance instruments that cover the spectral range from 1 to 2000 nm, but with no EUV observations [Woods et al., 2000a]. The SORCE XUV and FUV measurements will be similar to the TIMED XUV measurements and the UARS SOLSTICE FUV measurements, respectively. The goal of the SORCE measurements of the total solar irradiance (TSI) and the visible spectrum will have unprecedented accuracies of 0.01% and 0.03%, respectively. The SORCE launch is currently planned for the Summer 2002. These solar irradiance instruments on the TIMED and SORCE satellites have accurate pre-flight calibrations traceable to NIST and in-flight calibrations based on redundant channels, on-board reference detectors, or stellar observations. There are also other NASA, NOAA, and ESA missions being planned for solar cycle 24 that might include solar irradiance observations. These future missions will surely extend and improve our understanding of the solar irradiance over a longer

time scale and with a higher accuracy as technology and calibration standards continue to improve.

MODELS

Because of the limited amount of actual solar data, especially for the XUV and EUV regions, models of the solar variability are sometimes necessary for aeronomic studies. Some of the more commonly used solar irradiance models are empirical models, frequently called proxy models, that are derived using linear relations between a solar proxy and existing observations of the solar UV irradiance. These models typically use a commonly available solar measurement, such as the ground-based 10.7 cm radio solar flux (F10.7), that serves as the proxy for the solar irradiance at other wavelengths. The first widely used proxy model was the Hinteregger et al. [1981] model, which is based on the AE-E satellite observations and several sounding rocket measurements. The original proxies for this model were the chromospheric H I Lyman- β (102.6 nm) and the coronal Fe XVI (33.5 nm) emissions. As measurements of these emissions are not generally available, they are constructed from correlations with the daily F10.7 and its 81-day average, which have been available on a daily basis since 1947. This Hinteregger model is also referred to as SERF 1 by the Solar Electromagnetic Radiation Flux (SERF) subgroup of the World Ionosphere-Thermosphere Study. Richards et al. [1994] developed a similar F10.7 proxy model called EUVAC but increased the solar soft X-ray irradiances by a factor of 2 to 3 as compared to the SERF 1 model. In addition, Tobiska has developed several proxy models of the solar EUV irradiance: SERF 2 by Tobiska and Barth [1990], EUV91 by Tobiska [1991], EUV97 by Tobiska and Eparvier [1998], and the latest version, SOLAR2000, by Tobiska et al. [2000]. In addition to these simple proxy models, there are physical and semi-empirical models of the solar EUV irradiance: Fontenla et al. [1999], Warren et al. [1998a and 1998b], and Lean et al. [1982].

For developing or improving models of the irradiance, it is recommended that the solar UV irradiance variability be split into at least three components and that the different layers of the solar atmosphere are modeled separately [Woods et al., 2000b]. The three most important features on solar images to include in a solar UV irradiance model are the plages, active network, and quiet network [Lean et al., 1982; Worden, 1996]. For the more simple proxy models, which don't use results from solar images, the three most important components to include are the solar minimum value, the short-term variability, and the long-term variability [Woods et al., 2000b]. For modeling the solar UV irradiance, the chromosphere, transition region,

and corona emissions should be modeled separately as these emissions vary in different ways. A solution to include these different layers uniquely in a proxy model is to use three different proxies to represent each layer. For example, the NOAA Mg II core-to-wing ratio (available from 1978) is a good proxy for the chromospheric emissions and the photospheric continuum shortward of 200 nm, the composite H I Lyman- α (available from 1947) is a good proxy for the transition region emissions, and the F10.7 (available from 1947) is a good proxy for the coronal emissions [Woods *et al.*, 2000b]. The SOLAR2000 proxy model incorporates many of these ideas [Tobiska *et al.*, 2000].

REFERENCE SPECTRA FOR SOLAR CYCLE 22

For aeronomic studies, reference solar irradiance spectra representative of conditions during solar cycle 22 (1986-1996) are presented here. These reference spectra include spectra for solar minimum and maximum conditions and an example of 27-day rotational variability. These reference spectra are primarily established from actual observations; however, results from selected solar irradiance proxy models are used in creating and validating the reference solar spectra in the XUV and EUV range. These reference spectra are given in 1 nm intervals on 0.5 nm centers. This format is different than the commonly used 37 subdivisions for the solar EUV irradiance [e.g., Torr and Torr, 1985] because there are significant improvements in the accuracy of the atmospheric calculations when using the higher spectral resolution of 1 nm [Bailey, 1995].

The UARS solar measurements, which are limited to wavelengths longward of 115 nm, are adopted as the reference for the solar FUV irradiances presented here. The two UARS solar UV instruments are the Solar Ultraviolet Spectral Irradiance Monitor (SUSIM) [Brueckner *et al.*, 1993] and the Solar-Stellar Irradiance Comparison Experiment (SOLSTICE) [Rottman *et al.*, 1993]. While the two instruments are similar in that both are grating spectrometers with similar spectral resolution (0.1 nm) and both have pre-flight calibrations using NIST radiometric standards, they do utilize very different in-flight calibration techniques. The SUSIM uses redundant channels (optics) and on-board deuterium (D₂) lamps for its in-flight calibrations. The SOLSTICE uses about 20 early-type stars for its in-flight calibration. Both approaches have yielded similar results at the 3-10% level for the solar UV irradiance [Woods *et al.*, 1996].

The standard UARS solar product is the daily solar UV irradiance from about 115 nm to 420 nm in 1 nm intervals and on 0.5 nm centers. These UARS irradiance data are used for the FUV spectral region as the basis for the solar

minimum and maximum spectra listed in Table 2. The time periods for these reference spectra are discussed later in this section. They are tabulated in 1 nm intervals up to 200 nm with an absolute accuracy (standard 1- σ uncertainty) of about 10%. For longer wavelengths, two UARS reference spectra up to 420 nm are given by Woods *et al.* [1996]. The UARS irradiances are in good agreement, to better than 10%, of the World Meteorological Organization (WMO) reference spectrum [Fröhlich and London, 1986] above 210 nm, but the comparison between 210 nm and 200 nm, the shortest wavelength in the WMO spectrum, indicates that the UARS measurements are about 20% higher than the WMO spectrum. The validation of the UARS solar irradiances is extensive including several, nearly simultaneous measurements [Woods *et al.*, 1996], so the UARS irradiances are considered more accurate than the WMO reference spectrum.

There have been only a handful of solar EUV irradiance measurements during the past solar cycle (1986-1996). These measurements are from a few rocket measurements [Woods *et al.*, 1998a; Ogawa *et al.*, 1990; Ogawa and Judge, 1986] and a few observations in 1988 from the San Marco satellite [Schmidtke *et al.*, 1992; Worden *et al.*, 1996]. Donnelly [1987] refers to this period of sparse solar EUV measurements as the "EUV hole". Consequently, the last, more complete observation of the solar EUV irradiance by the AE-E satellite is often used for the reference EUV spectra [Hinteregger *et al.*, 1981, Torr and Torr, 1985]. Comparisons of the AE-E results to the more recent rocket measurements show differences by as much as a factor of 2 at some wavelengths [Woods *et al.*, 1998a]. However, it appears that the amount of variability recorded by AE-E is consistent with the limited set of recent measurements. The best characterization of the solar EUV is probably derived from combining the absolute levels of the recent, better calibrated, rocket instruments with the relative variability derived from the longer AE-E time series. Adopting this approach, the solar EUV irradiance measurement from a sounding rocket in 1994 [Woods *et al.*, 1998a] is used as the solar minimum reference spectrum, and the relative variability established by the AE-E measurements [Hinteregger *et al.*, 1981] is used to scale the solar minimum reference spectrum to a solar maximum spectrum. The SOLAR2000 model of the solar EUV irradiance [Tobiska *et al.*, 2000] incorporates both the recent rocket and past AE-E solar EUV irradiances; consequently, the SOLAR2000 model results are similar to these reference spectra. While the recent EUV measurements have uncertainties of 10-20%, the differences between these recent measurements and the AE-E and SOLAR2000 model results are 10-100%. It is difficult to assess and reconcile an absolute accuracy for the EUV reference spectra, but we

Table 2. A reference spectrum for solar cycle 22 minimum condition is listed in 1-nm intervals on 0.5 nm centers and at a solar distance of 1 AU. The values of the log (base-10) of the irradiance ($\log(E)$) are the irradiances in units of photons $s^{-1} cm^{-2}$. The 27-day variability and 11-year solar cycle variability ratios are also listed on the same wavelength grid. These ratios are the maximum value divided by the minimum value for the time period chosen for the ratio. These data are contained in a text file at ftp://laspftp.colorado.edu/pub/solstice/ref_min_27day_11yr.dat. As an example, the H I Lyman- α irradiance at 121.5 nm is located under the “@ $\lambda+1nm$ ” column in the “120.5” λ row with a value of 11.575, which is 3.75×10^{11} photons $s^{-1} cm^{-2}$.

λ (nm)	@ $\lambda+0nm$			@ $\lambda+1nm$			@ $\lambda+2nm$			@ $\lambda+3nm$			@ $\lambda+4nm$		
	Min log(E)	27D Var	11Y Var												
0.5	3.70	30.0	100.	6.00	6.0	20.0	7.00	3.0	10.0	7.455	1.66	4.70	7.834	1.56	3.29
5.5	8.282	1.42	2.26	8.288	1.44	2.37	8.409	1.37	2.11	8.247	1.41	2.12	8.395	1.31	1.80
10.5	8.000	1.27	1.68	7.902	1.22	1.64	7.739	1.22	1.61	7.755	1.22	1.63	8.218	1.40	2.05
15.5	8.206	1.54	2.98	8.542	1.28	1.72	9.192	1.36	1.86	8.827	1.49	2.45	8.782	1.57	3.11
20.5	8.422	1.61	3.77	8.285	1.65	4.28	8.645	1.46	2.46	8.392	1.42	2.26	8.778	1.48	2.49
25.5	8.986	1.51	2.71	8.381	1.64	4.10	8.723	1.57	3.27	8.590	1.72	6.21	8.393	1.49	2.47
30.5	9.873	1.24	1.57	9.045	1.48	2.41	8.799	1.74	7.28	8.807	1.74	7.23	8.849	1.48	2.41
35.5	8.750	1.53	2.77	8.892	1.53	2.79	8.381	1.10	1.17	8.025	1.10	1.17	7.980	1.17	1.43
40.5	8.215	1.17	1.43	8.003	1.73	6.50	7.976	1.10	1.17	8.268	1.30	1.60	7.957	1.10	1.17
45.5	7.923	1.22	1.64	8.471	1.33	1.75	8.099	1.22	1.64	8.337	1.21	1.59	8.628	1.59	3.65
50.5	8.532	1.19	1.51	8.061	1.21	1.59	8.093	1.56	3.19	8.192	1.21	1.59	8.048	1.16	1.38
55.5	8.700	1.17	1.42	8.172	1.19	1.52	8.156	1.22	1.64	8.903	1.24	1.71	8.286	1.16	1.41
60.5	8.734	1.49	2.49	8.403	1.16	1.38	9.024	1.21	1.51	8.410	1.22	1.64	7.823	1.16	1.38
65.5	7.691	1.21	1.58	7.682	1.16	1.38	7.688	1.17	1.44	8.224	1.20	1.48	8.077	1.25	1.61
70.5	8.541	1.16	1.39	8.174	1.18	1.47	8.012	1.24	1.72	8.133	1.24	1.72	8.229	1.24	1.72
75.5	8.443	1.21	1.58	8.865	1.19	1.50	8.735	1.40	2.10	8.964	1.25	1.61	8.663	1.18	1.48
80.5	8.641	1.24	1.72	8.702	1.24	1.72	8.876	1.24	1.72	9.150	1.19	1.51	8.981	1.24	1.72
85.5	9.032	1.24	1.72	9.063	1.24	1.72	9.144	1.24	1.72	9.207	1.24	1.72	9.296	1.24	1.72
90.5	9.375	1.24	1.71	9.269	1.23	1.68	8.821	1.23	1.70	8.777	1.22	1.65	8.632	1.23	1.67
95.5	8.438	1.17	1.44	8.460	1.17	1.44	9.699	1.20	1.54	8.775	1.18	1.45	8.968	1.18	1.45
100.5	8.582	1.17	1.44	8.649	1.17	1.44	9.568	1.24	1.71	9.589	1.23	1.69	8.802	1.17	1.44
105.5	8.734	1.17	1.44	8.718	1.17	1.43	8.748	1.17	1.43	8.975	1.17	1.44	8.807	1.17	1.44
110.5	8.839	1.17	1.44	8.856	1.10	1.17	8.837	1.19	1.50	8.793	1.10	1.17	8.628	1.10	1.17
115.5	8.847	1.10	1.17	8.904	1.10	1.17	9.473	1.19	1.51	8.963	1.10	1.17	9.447	1.17	1.39
120.5	9.875	1.27	1.73	11.575	1.22	1.64	9.499	1.17	1.33	9.346	1.24	1.37	9.231	1.21	1.37
125.5	9.220	1.16	1.32	9.361	1.21	1.50	9.124	1.17	1.29	9.047	1.16	1.25	9.098	1.18	1.38
130.5	10.020	1.15	1.29	9.255	1.12	1.19	9.132	1.14	1.25	10.057	1.22	1.57	9.088	1.12	1.25
135.5	9.453	1.12	1.23	9.262	1.14	1.26	9.297	1.12	1.24	9.300	1.11	1.21	9.700	1.22	1.60
140.5	9.652	1.17	1.43	9.464	1.10	1.22	9.505	1.10	1.20	9.572	1.10	1.21	9.563	1.09	1.20
145.5	9.599	1.09	1.20	9.695	1.11	1.20	9.799	1.07	1.16	9.809	1.09	1.17	9.766	1.08	1.17
150.5	9.817	1.08	1.16	9.853	1.08	1.16	9.946	1.10	1.21	9.998	1.10	1.20	10.228	1.16	1.31
155.5	10.162	1.12	1.24	10.182	1.08	1.16	10.141	1.06	1.16	10.128	1.07	1.15	10.134	1.06	1.13
160.5	10.185	1.06	1.15	10.258	1.05	1.14	10.320	1.06	1.14	10.359	1.06	1.16	10.406	1.10	1.17
165.5	10.613	1.09	1.12	10.467	1.04	1.07	10.531	1.07	1.12	10.592	1.04	1.06	10.710	1.05	1.07
170.5	10.772	1.04	1.08	10.769	1.05	1.11	10.808	1.05	1.09	10.815	1.05	1.08	10.907	1.05	1.07
175.5	10.999	1.05	1.08	11.037	1.04	1.07	11.118	1.04	1.08	11.168	1.05	1.08	11.159	1.05	1.08
180.5	11.245	1.07	1.12	11.325	1.08	1.15	11.311	1.05	1.09	11.345	1.05	1.09	11.283	1.04	1.08
185.5	11.343	1.04	1.08	11.403	1.05	1.09	11.469	1.04	1.09	11.496	1.04	1.09	11.548	1.04	1.10
190.5	11.567	1.04	1.08	11.608	1.04	1.09	11.638	1.04	1.09	11.521	1.03	1.08	11.744	1.04	1.08
195.5	11.735	1.04	1.08	11.791	1.04	1.08	11.799	1.04	1.07	11.805	1.03	1.06	11.843	1.03	1.06

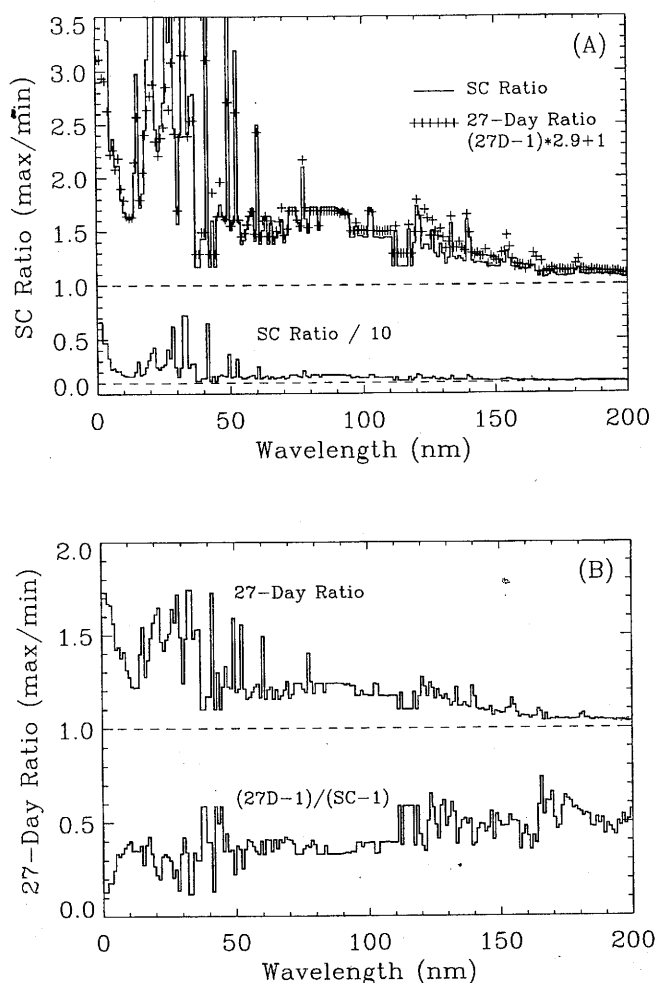


Figure 2. The variation of the solar irradiance for solar cycle 22 (SC 22) and for a 27-day period near 1992/032 are shown in panels A and B, respectively. These results used the UARS SOLSTICE measurements in 1992 and 1996 for the FUV and a combination of rocket, SNOE, and model results for the EUV and XUV. The plus symbols in panel A are the 27-day variability with a scaling factor of 2.9 so that the short-term variability is the same level as the long-term variability at 121.5 nm (H I Lyman- α). The ratio of the 27-day and SC variability, as shown in panel B, varies with wavelength due to the emissions being from different layers in the solar atmosphere.

suggest an accuracy of 30% for the EUV range (30-120 nm).

The XUV spectral region has even fewer measurements because of the technical difficulties for XUV optics and detectors. The primary knowledge of the solar XUV is from several rocket measurements [Feng *et al.*, 1989; Bailey *et al.*, 1999], the SOLRAD satellite measurements shortward of 10 nm [Kreplin, 1970; Kreplin and Horan, 1992], the GOES 1-8 Å measurements, the Yohkoh solar imaging

experiment shortward of 10 nm [Acton *et al.*, 1999], the SOHO Solar EUV Monitor (SEM) daily results in the 26-34 nm bandpass [Judge *et al.* 1998; Ogawa *et al.*, 1998], and the SNOE Solar XUV Photometer (SXP) daily observations shortward of 20 nm (2-7 nm, 6-19 nm, and 17-20 nm bandpasses) [Bailey *et al.*, 2000]. The SNOE SXP and SOHO SEM measurements provide the most recent and most accurate knowledge of the solar XUV irradiance. However, these instruments have broad spectral resolution (~ 7 nm), so the solar XUV irradiance reference is chosen to be the SOLAR2000 model in 1 nm intervals but scaled to match the SNOE and SOHO results. Bailey *et al.* [2000] report that the SNOE XUV irradiances are a factor of 4 higher than the AE-E solar reference spectra [Hinteregger *et al.*, 1981]. In support of this increase, Solomon *et al.* [2001] show that the photoelectron flux measurements are consistent with photoelectron calculations that use a scaling factor of 4 for the solar irradiance shortward of 20 nm. This scaling factor is consistent with several other results from photoelectron and atmospheric studies [e.g., Roble, 1976; Oster, 1983; Richards and Torr, 1984; Buonsanto *et al.*, 1995]. The SNOE SXP and SOHO SEM irradiances have a 10-20% uncertainty. The redistribution of the low-resolution irradiances into higher spectral resolution introduces additional uncertainty, so we estimate the total uncertainty for the reference solar XUV irradiance to be about 40%.

The largest 27-day variability observed during the UARS mission occurred on 1992/032 (year / day of year), and this period is used to define a reference 27-day variability spectrum as shown in Figure 2. The solar rotational variability is strongly dependent on wavelength. The source of the emission in the solar atmosphere, which affects the active network and plage contribution to the emission, appears to be the key reason for the spectral differences. While essentially all of the emissions shortward of 200 nm appear to increase and decrease together during a solar rotation, the coronal and transition region emissions vary the most, and the chromospheric emissions and photospheric continuum vary the least. For cases when the solar observations are not available, this reference 27-day variability spectrum could be used to study aeronomic observations over a short-term period of days. As indicated by the H I Lyman- α variability in Figure 1, it may be necessary to scale this reference 27-day variability downward by as much as a factor of 6 or upward by as much as a factor of 2 when studying a specific aeronomic observation.

The solar minimum and maximum reference spectra are chosen centered on 1996/108 and 1992/032, respectively. These solar cycle spectra are obtained by averaging over 27-days to represent the mean value during a solar rotation. The solar irradiance spectra for these two periods are listed

in Table 2 for a solar distance of 1 AU. The solar 10.7 cm radio fluxes (F10.7), averaged over these two 27-day periods, are 71 and 212 for solar minimum and maximum, respectively. Because of the 27-day averaging, the 11-year variability factors are reduced from a ratio taken without any averaging. For studies needing the expected extreme values of the 11-year variability during solar cycle 22, one can multiply the 27-day variability factor and the 11-year variability factor, both given in Table 2 in 1 nm intervals. For example, the extreme 11-year variability of the H I Lyman- α emission at 121.5 nm is 2.0 (1.22 x 1.64).

The long-term variability has a spectral function similar, but not identical, to the short-term variability. The ratio of the solar maximum and minimum spectra, given in Figure 2, shows the wavelength dependence of the irradiance over the 11-year solar cycle. Our reference 27-day rotational variability is compared to the reference long-term variability, and this comparison, which is also included in Figure 2, indicates that this specific short-term variability is about a factor of 2 to 3 smaller. It is important to note that this ratio of 1/3 is appropriate for the upper chromospheric and transition region emissions, such as for H I Lyman- α , but a ratio of 1/2 and 1/4 is more appropriate for the lower chromospheric and coronal emissions, respectively. This result is expected because the different emissions have different contributions to their long-term variations from the active network features on the Sun, which causes their long-term variability relative to their short-term variability to be different [Woods *et al.*, 2000b]. Because of the different behavior of the long-term variations relative to the short-term variations as a function of wavelength, the reference 27-day variability should not be scaled to study aeronomic observations over a long-term period of several months or years. Obviously, the long-term variability derived from the solar minimum and maximum spectra is more appropriate for aeronomic studies over a long-term period.

SUMMARY

The solar UV radiation important for aeronomic studies is primarily the irradiance shortward of 200 nm. The solar variabilities important for most aeronomic studies are the 27-day solar rotation and the 11-year solar cycle. Both of these variations have a similar spectral shape, but the 11-year solar cycle variation is about a factor of 2 to 3 larger than the largest 27-day solar rotation variation. The photospheric continuum at wavelengths longward of 260 nm varies the least, by probably only 0.1% [Fontenla *et al.*, 1999]. The continuum variation sharply rises shortward of 260 nm, and an even larger rise in the solar variability is observed below the Al ionization edge at 207 nm. The

continuum at 200 nm has a solar cycle variation of 6%, and then the continuum variation slowly rises to 25% near 132 nm. The emissions from Ca II near 395 nm and Mg II near 280 nm are the brightest emissions from the chromosphere. There are also many other chromospheric emissions between 91 nm and 182 nm, and most of these chromospheric emissions vary by about 40% over the solar cycle. The emission from H I at 121.6 nm and He II at 30.4 nm are the brightest emissions from the transition region. There are also several transition region emissions between 23 nm and 155 nm. Most of these transition region emissions vary by about 70% over the solar cycle. The coronal emissions are primarily shortward of 63 nm, and they vary the most. The lower temperature corona emissions, like Mg X, vary by a factor of 2 over the solar cycle, and the higher temperature coronal emissions, like Fe XVI, vary by a factor of 8. In terms of the total energy variation, the chromospheric emissions contribute more than the transition region emissions, which contribute more than the coronal emissions. However, most atmospheric processes have a strong wavelength dependence, thus the solar variability at the appropriate wavelength needs to be considered for each atmospheric process. While the reference spectra included here represent the current understanding of the solar UV irradiance during solar cycle 22, there are upcoming future satellite missions that should provide even better accuracy for the solar UV irradiances and thus further refine on-going and future aeronomy research.

Acknowledgments. We thank our UARS SOLSTICE and rocket experiment teams for providing operations and data processing support in producing solar irradiance products from those experiments. We especially thank Frank Eparvier and Don Woodraska for their many useful comments about this paper. This work is supported by NASA contracts NAS5-97145 and NAS5-97045 and JHU/APL contract JH774017. The reference solar spectra can be obtained as a text data file called `ref_min_27day_11yr.dat` from the LASP FTP site (<ftp://laspftp.colorado.edu/pub/solstice/>), and this file can be read using the IDL code called `read_dat.pro` also at the LASP FTP site.

REFERENCES

- Acton, L. W., D. C. Weston, and M. E. Bruner, Deriving solar x-ray irradiance from Yohkoh observations, *J. Geophys. Res.*, 104, 14827, 1999.
- Babcock, H. W., The topology of the Sun's magnetic field and the 22-year cycle, *Ap. J.*, 133, 572, 1961.
- Bailey, S. M., *Response of the Upper Atmosphere to Variations in the Solar Soft X-ray Irradiance*, dissertation, Univ. of Colo., Boulder, 1995.
- Bailey, S. M., T. N. Woods, L. R. Canfield, R. Korde, C. A. Barth, S. C. Solomon, and G. J. Rottman, Sounding rocket meas-

- urements of the solar soft x-ray irradiance, *Solar Phys.*, 186, 243, 1999.
- Bailey, S. M., T. N. Woods, C. A. Barth, S. C. Solomon, L. R. Canfield, and R. Korde, Measurements of the solar soft x-ray irradiance from the Student Nitric Oxide Explorer: first analysis and underflight calibrations, *J. Geophys. Res.*, 105, 27,179, 2000.
- Baum, W. A., F. S. Johnson, J. J. Oberly, E. E. Rockwood, C. V. Strain, and R. Tousey, Solar ultraviolet spectrum to 88 kilometers, *Phys. Rev.*, 70, 781, 1946.
- Brekke, P., G. J. Rottman, J. Fontenla, and P. G. Judge, The ultraviolet spectrum of a 3B class flare observed with SOLSTICE, *Astrophys. J.*, 468, 418, 1996.
- Brasseur, G. and S. Solomon, *Aeronomy of the Middle Atmosphere: Chemistry and Physics of the Stratosphere and Mesosphere*, Dordrecht, Boston, 1986.
- Brueckner, G.E., K.L. Edlow, L.E. Floyd, J.L. Lean, and M.E. VanHoosier, The Solar Ultraviolet Spectral Irradiance Monitor (SUSIM) Experiment on board the Upper Atmospheric Research Satellite (UARS), *J. Geophys. Res.*, 98, 10695, 1993.
- Buonsanto, M. J., P. G. Richards, W. K. Tobiska, S. C. Solomon, Y.-K. Tung, and J. A. Fennelly, Ionospheric electron densities calculated using different EUV flux models and cross sections: Comparison with radar data, *J. Geophys. Res.*, 100, 14569, 1995.
- Chamberlain, J. W., *Theory of Planetary Atmospheres: An Introduction to Their Physics and Chemistry*, Academic Press, New York, 1978.
- Donnelly, R. F., Gaps between solar UV & EUV radiometry and atmospheric sciences, in *Solar Radiative Output Variation*, edited by P. Foukal, pp. 139-142, Cambridge Research and Instrumentation Inc, Boulder, Colorado, 1987.
- Feng, W. H. S. Ogawa, and D. L. Judge, The absolute solar soft x ray flux in the 20 - 100Å region, *J. Geophys. Res.*, 94, 9125, 1989.
- Feynman, J. and S. B. Gabriel, Period and phase of the 88_{yr} solar cycle and the Maunder Minimum: Evidence for a chaotic Sun, *Solar Phys.*, 127, 393, 1990.
- Fontenla, J. M., O. R. White, P. A. Fox, E. H. Avrett, and R. L. Kurucz, Calculation of solar irradiances. I. Synthesis of the solar spectrum, *Astrophys. J.*, 518, 480, 1999.
- Fröhlich, C., and J. London, *Revised Instruction Manual on Radiation Instruments and Measurements*, WMO/TD-No. 149, World Metrological Organization, Geneva, 1986.
- Hall, L. A., and H. E. Hinteregger, Solar radiation in the extreme ultraviolet and its variation with solar rotation, *J. Geophys. Res.*, 75, 6959, 1970.
- Harvey, K. L., and O. R. White, Magnetic and radiative variability of solar surface structures. 1. Image decomposition and magnetic-intensity mapping, *Astrophys. J.*, 515, 812, 1999.
- Hinteregger, H. E., D. E. Bedo, and J. E. Manson, The EUV spectrophotometer on Atmosphere Explorer, *Radio Science*, 8, 349, 1973.
- Hinteregger, H. E., K. Fukui, and B. R. Gilson, Observational, reference and model data on solar EUV, from measurements on AE-E, *Geophys. Res. Letters*, 8, 1147, 1981.
- Judge, D. L., D. R. McMullin, H. S. Ogawa, D. Hovestadt, B. Klecker, M. Hilchenbach, E. Möbius, L. R. Canfield, R. E. Vest, R. Watts, C. Tarrío, and M. Kühne, First solar EUV irradiances obtained from SOHO by the CELIAS/SEM, *Solar Phys.*, 177, 161, 1998.
- Kreplin, R. W., The solar cycle variation of soft x-ray emission, *Ann. Geophys.*, 26, 567, 1970.
- Kreplin, R. W. and D. M. Horan, Variability of x-ray and EUV solar radiation in solar cycles 20 and 21, in *Proceedings of the Workshop on the Solar Electromagnetic Radiation Study for Solar Cycle 22*, edited by R. F. Donnelly, pp. 405-425, NOAA, Boulder, 1992.
- Layden, A. C., P. A. Fox, J. M. Howard, A. Sarajedini, K. H. Schatten, and S. Sofia, Dynamo-based scheme for forecasting the magnitude of solar activity cycles, *Solar Phys.*, 132, 1, 1991.
- Lean, J. L., W. C. Livingston, D. F. Heath, R. F. Donnelly, A. Skumanich, and O. R. White, A three-component model of the variability of the solar ultraviolet flux 145-200 nm, *J. Geophys. Res.*, 87, 10307, 1982.
- Lean, J., Solar ultraviolet irradiance variations: A review, *J. Geophys. Res.*, 92, 839, 1987.
- Lean, J., Variations in the Sun's radiative output, *Reviews of Geophysics*, 29, 505, 1991.
- Levy, E. H., The solar cycle and dynamo theory, in *The Solar Cycle*, edited by K. L. Harvey, pp. 139-149, ASP Conference Series 27, 1992.
- Maunder, E. W., The Sun and sunspots, 1820-1920, *Mon. Not. Roy. Astron. Soc.*, 82, 534, 1922.
- Meier, R. R., Solar Lyman series line profiles and atomic hydrogen excitation rates, *Astrophys. J.*, 452, 462, 1995.
- Ogawa, H. S. and D. L. Judge, Absolute solar flux measurements shortward of 575 Å, *J. Geophys. Res.*, 91, 7089, 1986.
- Ogawa, H. S., L. R. Canfield, D. McMullin, and D. L. Judge, Sounding rocket measurement of the absolute solar EUV flux utilizing a silicon photodiode, *J. Geophys. Res.*, 95, 4291, 1990.
- Ogawa, H. S., D. L. Judge, D. R. McMullin, and P. Gangopadhyay, First-year continuous solar EUV irradiance from SOHO by the CELIAS/SEM during 1996 solar minimum, *J. Geophys. Res.*, 10, 1, 1998.
- Oster, L., Solar irradiance variations, 2. Analysis of the extreme ultraviolet spectrometer measurements onboard the Atmospheric Explorer E satellite, *J. Geophys. Res.*, 88, 9037, 1983.
- Pap, J. M., C. Fröhlich, H. S. Hudson, and S. K. Solanki (editors), *The Sun as a Variable Star: Solar and Stellar Irradiance Variations*, Cambridge University Press, Cambridge, 1994.
- Reeves, E. M. and W. H. Parkinson, An atlas of extreme-ultraviolet spectroheliograms from OSO-IV, *Astrophys. J. Supplement*, 181, 1, 1970.
- Richards, P. G. and D. G. Torr, An investigation of the consis-

- tency of the ionospheric measurements of the photoelectron flux and solar EUV flux, *J. Geophys. Res.*, *89*, 5625, 1984.
- Richards, P. G., J. A. Fennelly, and D. G. Torr, EUVAC: A solar EUV flux model for aeronomic calculations, *J. Geophys. Res.*, *99*, 8981, 1994.
- Roble, R. G., Solar EUV variation during a solar cycle as derived from ionospheric modeling considerations, *J. Geophys. Res.*, *81*, 265, 1976.
- Rottman, G. J., Results from space measurements of solar UV and EUV flux, in *Solar Radiative Output Variation*, edited by P. Foukal, pp. 71-86, Cambridge Research and Instrumentation Inc, Boulder, 1987.
- Rottman, G. J., T. N. Woods, and T. P. Sparr, Solar Stellar Irradiance Comparison Experiment 1: 1. Instrument design and operation, *J. Geophys. Res.*, *98*, 10667, 1993.
- Schmidtke, G., T. N. Woods, J. Worden, H. Doll, S. C. Solomon, and G. J. Rottman, Solar EUV irradiance from the San Marco ASSI: a reference spectrum, *Geophys. Res. Letters*, *19*, 2175, 1992.
- Schrijver, C. J., Radiative fluxes from the outer atmosphere of a star like the Sun - A construction kit, *Astron. Astrophys.*, *189*, 163, 1988.
- Schühle, U., K. Wilhelm, J. Hollandt, P. Lemaire, and A. Pauluhn, Radiance variations of the quiet Sun at far-ultraviolet wavelengths, *Astron. Astrophys.*, *354*, L71, 2000.
- Solomon, S. C., S. M. Bailey, and T. N. Woods, Effect of solar soft x-rays on the lower ionosphere, *Geophys. Res. Lett.*, *28*, 2149, 2001.
- Spörer, G., Beobachtungen von Sonnenflecken in den Jahren 1885 bis 1893, *Pub. Astrophys. Obs. Potsdam*, *10*, 144, 1894.
- Tobiska, W. K. and C. A. Barth, A solar EUV flux model, *J. Geophys. Res.*, *95*, 8243, 1990.
- Tobiska, W. K., Revised solar extreme ultraviolet flux model, *J. Atmos. Terr. Phys.*, *53*, 1005, 1991.
- Tobiska, W. K., Recent solar extreme ultraviolet irradiance observations and modeling: A review, *J. Geophys. Res.*, *98*, 18879, 1993.
- Tobiska, W. K., and F. G. Eparvier, EUV97: Improvements to EUV irradiance modeling in the soft x-rays and FUV, *Solar Phys.*, *177*, 147, 1998.
- Tobiska, W. K., T. N. Woods, F. G. Eparvier, R. Viereck, L. Floyd, D. Bouwer, G. J. Rottman, and O. R. White, The SOLAR2000 empirical solar irradiance model and forecast tool, *J. Atmos. and Sol. Terr. Phys.*, *62*, 1233, 2000.
- Torr, M. R., and D. G. Torr, Ionization frequencies for solar cycle 21: revised, *J. Geophys. Res.*, *90*, 6675, 1985.
- Warren, H. P., J. T. Mariska, and J. Lean, A new reference spectrum for the EUV irradiance of the quiet Sun: 1. Emission measure formulation, *J. Geophys. Res.*, *103*, 12077, 1998a.
- Warren, H. P., J. T. Mariska, and J. Lean, A new reference spectrum for the EUV irradiance of the quiet Sun: 2. Comparisons with observations and previous models, *J. Geophys. Res.*, *103*, 12091, 1998b.
- White, O. R. (editor), *The Solar Output and Its Variation*, Colorado Ass. Univ. Press, Boulder, 1977.
- Woods, T. N., D. K. Prinz, J. London, G. J. Rottman, P. C. Crane, R. P. Cebula, E. Hilsenrath, G. E. Brueckner, M. D. Andrews, O. R. White, M. E. VanHoosier, L. E. Floyd, L. C. Herring, B. G. Knapp, C. K. Pankratz, and P. A. Reiser, Validation of the UARS solar ultraviolet irradiances: Comparison with the ATLAS 1 and 2 measurements, *J. Geophys. Res.*, *101*, 9541-9569, 1996.
- Woods, T. N., G. J. Rottman, S. M. Bailey, S. C. Solomon, and J. Worden, Solar extreme ultraviolet irradiance measurements during solar cycle 22, *Solar Physics*, *177*, 133-146, 1998a.
- Woods, T. N., F. G. Eparvier, S. M. Bailey, S. C. Solomon, G. J. Rottman, G. M. Lawrence, R. G. Roble, O. R. White, J. Lean, and W. K. Tobiska, TIMED Solar EUV Experiment, *SPIE Proceedings*, *3442*, 180-191, 1998b.
- Woods, T., G. Rottman, J. Harder, G. Lawrence, B. McClintock, G. Kopp, and C. Pankratz, Overview of the EOS SORCE mission, *SPIE Proceedings*, *4135*, 192, 2000a.
- Woods, T. N., W. K. Tobiska, G. J. Rottman, and J. R. Worden, Improved solar Lyman α irradiance modeling from 1947 through 1999 based on UARS observations, *J. Geophys. Res.*, *105*, 27,195 2000b.
- Worden, J. R., *A Three Component Proxy Model for the Solar Far Ultraviolet Irradiance*, dissertation, Univ. of Colo., Boulder, 1996.
- Worden, J., T. N. Woods, G. J. Rottman, G. Schmidtke, H. Tai, H. G. Doll, and S. C. Solomon, Calibration of the San Marco Airglow-Solar Spectrometer Instrument in the extreme ultraviolet, *Optical Eng.*, *35*, 554, 1996.
- Worden, J. R., O. R. White, and T. N. Woods, Evolution of chromospheric structures derived from Ca II K spectroheliograms: implications for solar ultraviolet irradiance variability, *Astrophys. J.*, *496*, 998, 1998.
- Worden, J., T. N. Woods, W. M. Neupert, and J.P. Delaboundiniere, Evolution of chromospheric structures: How chromospheric structures contribute to the solar He II 30.4 nanometer irradiance and variability, *Astrophys. J.*, *511*, 965, 1999.

Thomas N. Woods and Gary J. Rottman, Laboratory for Atmospheric and Space Physics, University of Colorado, 1234 Innovation Dr., Boulder, CO 80303